

# Statistical power for cluster analysis

Edwin S. Dalmaiher, Camilla L. Nord, & Duncan E. Astle

*MRC Cognition and Brain Sciences Unit, University of Cambridge, Cambridge, United Kingdom*

## Corresponding author

Dr Edwin S. Dalmaiher, MRC Cognition and Brain Sciences Unit, 15 Chaucer Road, Cambridge, CB2 7EF, United Kingdom. Telephone: 0044 1223 769 447. Email: [edwin.dalmaiher@mrc-cbu.cam.ac.uk](mailto:edwin.dalmaiher@mrc-cbu.cam.ac.uk)

## Acknowledgements

ESD and DEA are supported by grant TWCF0159 from the Templeton World Charity Foundation to DEA. CLN is supported by an AXA Fellowship. All authors are supported by the UK Medical Research Council.

## Manuscript details

Word count

**Abstract: 236 words**

Introduction: 700

Methods: 1760

Results: 2084

Discussion: 624

**Total: 5168 words**

Figures: 11

Tables: 3

## Abstract

Cluster algorithms are gaining in popularity due to their compelling ability to identify discrete subgroups in data, and their increasing accessibility in mainstream programming languages and statistical software. While researchers can follow guidelines to choose the right algorithms, and to determine what constitutes convincing clustering, there are no firmly established ways of computing a priori statistical power for cluster analysis. Here, we take a simulation approach to estimate power and classification accuracy for popular analysis pipelines. We systematically varied cluster size, number of clusters, number of different features between clusters, effect size within each different feature, and cluster covariance structure in generated datasets. We then subjected these datasets to common dimensionality reduction approaches (none, multi-dimensional scaling, or uniform manifold approximation and projection) and cluster algorithms (k-means, hierarchical agglomerative clustering with Ward linkage and Euclidean distance, or average linkage and cosine distance, HDBSCAN). Furthermore, we simulated additional datasets to explore the effect of sample size and cluster separation on statistical power and classification accuracy. We found that clustering outcomes were driven by large effect sizes or the accumulation of many smaller effects across features, and were mostly unaffected by differences in covariance structure. Sufficient statistical power can be achieved with relatively small samples ( $N=20$  per subgroup), provided cluster separation is large ( $\Delta=4$ ). Finally, we discuss whether fuzzy clustering (c-means) could provide a more parsimonious alternative for identifying separable multivariate normal distributions, particularly those with lower centroid separation.

**Keywords:** statistical power, dimensionality reduction, cluster analysis, simulation, sample size, effect size, covariance

## Introduction

Cluster analyses are unsupervised algorithms that aim to delineate subgroups in datasets. They have steadily gained in popularity, for example to identify protein communities involved in cancer metastasis (Jonsson et al., 2006), responder types to cancer treatment (De La Monte et al., 1986), brain types (Bathelt et al., 2017), and behavioural phenotypes (Astle et al., 2019; Bathelt et al., 2018; Benjamins et al., 2019; Rennie et al., 2019). This increase is in part due to improvements in computational power, but also in the availability of user-friendly packages for open-source platforms Python (Pedregosa et al., 2011) and R (Hennig, 2020), and built-in options in proprietary software Matlab, Stata, and SPSS.

While cluster algorithms are increasingly accessible, what constitutes a “cluster” remains a complex philosophical question (Hennig, 2015), and potentially a practical issue. Take Marmite, for example, where there seems to be a very clear separation between people’s opinions: one (perhaps smaller) subgroup likes it, and another absolutely does not, while no lukewarm opinions seem to exist. Unfortunately, many systems do not work in this discrete way. For instance, while the level of serum testosterone in women can be diagnostic of polycystic ovary syndrome, the distributions of patients and controls partially overlap (Handelsman et al., 2017). Furthermore, this type of partial overlap can be introduced or exaggerated by measurement error. Finally, subgroups can present with similar central tendencies, but entirely different covariance structures.

Most clustering tutorials and method comparisons do not consider these complexities. Instead, they provide idealised data from simulated strongly separated high-dimensional “blobs” (Figure 1, left column), or from features measured in clearly distinct groups such as different species of flowers (Fisher, 1936) (Figure 1, middle column). Even studies aimed at identifying factors that impact cluster algorithm performance have used unlikely large cluster separation (Arbelaitz et al., 2013; Dubes, 1987). Unlike these examples, real data frequently takes the form of multivariate normal distributions that are not particularly well separated (Figure 1, right column). In this scenario, observations may be sampled from categorically distinct groups, but it is unclear whether cluster algorithms can always recognise this.

Scientists have not only increased their usage of statistical tools from the machine learning shed, but have also increasingly become aware of the potential issue of low statistical power: the likelihood that a test can correctly rejecting a null hypothesis. In fact, it has been suggested “that most published research findings are false” (Ioannidis, 2005). For example, the majority of neuroscience studies have a very low power with a median 21% (i.e. only 21 out of 100 true effects would be detected) (Button et al., 2013), although it has been suggested this varies notably by sub-discipline (Nord et al., 2017). To help prevent the proliferation of low-power studies in the era of modern statistics (“data science”), it is important that the statistic power of tools like cluster analysis is investigated.



**Figure 1** – This figure shows three datasets in the top row, each made up out of 150 observations that fall in three equally sized clusters. While the datasets are made up of 4 features, the plotted data is a two-dimensional projection through multi-dimensional scaling (MDS). The left column presents simulated “blobs” as they are commonly used in clustering tutorials, the middle column presents the popular Iris dataset, and the right presents more realistic multivariate normal distributions. The bottom row presents the outcome of k-means clustering, showing good classification accuracy for all datasets, but only reliable cluster detection (silhouette coefficient of 0.5 or over) for blobs and the Iris dataset, but not the more realistic scenario.

Here, we explore what factors affect cluster algorithms’ ability to delineate subgroups. We simulate datasets in which we systematically vary covariance structure, relative subgroup size, number, and separation. In addition, we investigate the effects of dimensionality reduction algorithms that project high-dimensional data into a lower-dimensional space.

After simulating data, and optionally reducing its dimensionality, we subjected it to popular cluster algorithms: k-means (Lloyd, 1982), (hierarchical) agglomerative clustering (Ward, 1963), and HDBSCAN (McInnes et al., 2017). This allowed us to map the effects of aforementioned factors, and to compute the statistical power as a function of simulated sample and effect sizes.

Finally, we note that “hard” clustering methods like k-means assign observations to only one cluster. However, particularly in multivariate normal distributions with some overlap, this leads to overconfident assignment of observations that lie roughly between two centroids. A solution implemented in some algorithms, notably HDBSCAN, is to leave some observations unassigned.

However, this does not do justice to the real situation, which is that we can have some confidence that observations halfway between centroids can be assigned to either cluster, but not to any other cluster. Fuzzy clustering allows for exactly this kind of proportionally shared assignment, and hence is perhaps more parsimonious with real data. To explore whether this translates into better statistical power, we compare the hard k-means and the fuzzy c-means algorithms.

## Methods

### Simulation

Data was simulated in Python (Van Rossum & Drake, 2011) (for a tutorial, see (Dalmajjer, 2017)), using the NumPy package's (Oliphant, 2007) to sample from multivariate normal distributions with predefined covariance and feature means within each subgroup. Generated datasets constituted 1000 observations and 15 features, with defined mean vectors (see below), and standard deviations of 1 within each feature. The number of subgroups was 2 with unequal group size (10/90%), 2 with equal group size (50/50%), or 3 with equal group size (33/34/33%). Within each simulation, within-feature differences were generated with Cohen's  $d$  values of 0.3, 0.5, 0.8, 1.3, or 2.1, and the number of different features was 1, 5, 10, or 15.

For two-cluster datasets, centroids (mean vectors) were determined by subtracting half the intended Cohen's  $d$  from one cluster, and adding the same value to the other within each feature. The order of addition and subtraction was shuffled within each feature. For three-cluster datasets, one cluster was assigned a mean vector of zeros (the "middle" cluster). The other two clusters had the intended Cohen's  $d$  added or subtracted within each feature, again with shuffled order within each feature.

Covariance structures were generated in three different ways: no covariance with values of 0 for all non-diagonal relations; uniform random values between -0.3 and 0.3; or with imposed 3 or 4 factor structure with uniform random values between -0.9 and -0.4 or between 0.4 and 0.9 within each factor, and between -0.3 and 0.3 for relations between variables in different factors. We also included two types of datasets with different covariance structures between subgroups, one with different underlying factor structures (3 and 4 factors; or 3 and 4 and no factors), and one simply with different covariance structures (random and random; or random and random and no covariance).

To compute statistical power and accuracy, further simulations were run to generate datasets of 10, 20, 40, 80, or 160 observations and 2 features. These datasets were constructed with two unequally sized (10/90%), two equally sized, three equally sized, or four equally sized subgroups (multivariate normal distributions with standard deviations of one); all with equidistant means at centroid separations of  $\Delta=1$  to 10. For each combination of variables, new data was generated in 100 iterations, and then analysed with k-means, HDBSCAN, or c-means (see below).

Finally, to compare the power and sensitivity of k-means and c-means, datasets of 120 observations and 2 (uncorrelated) features were simulated with one, two, three, or four equally sized and equidistant multivariate normal distributions ( $SD=1$ ). Their separations varied from  $\Delta=1$  to 10, and they were analysed with k-means and c-means (see below).

## Open Code and Data

All code and simulated data used for this manuscript can be found on GitHub, from where it can be freely accessed and downloaded: [www.github.com/esdalmajer/cluster\\_power](https://www.github.com/esdalmajer/cluster_power)

## Dimensionality reduction

Cluster analysis is usually performed on high-dimensional data, i.e. with many measured features per observation. While it is possible to apply clustering algorithms directly, the “curse of dimensionality” entails that this approach is unlikely to yield strong results (Bellman, 1957). Instead, many opt for projecting high-dimensional data into a lower-dimensional space. One option for this is principal component analysis (PCA), but extracting only a few components risks removing meaningful variance. Instead, data can be projected in two-dimensional space with limited loss of information with multi-dimensional scaling (Kruskal, 1964) (MDS), a technique that aims to retain inter-observation distances in original data in a lower-dimensional projection. Finally, algorithms such as t-stochastic neighbour embedding (t-SNE) (Van der Maaten & Hinton, 2008) and uniform manifold approximation and projection (UMAP) (McInnes et al., 2018) non-linearly reduce dimensionality, effectively retaining local inter-sample distances while exaggerating global distances. An additional advantage of these techniques is that data projected into two or three dimensions can be plotted, and thus visually inspected for oddities, and perhaps even provide an rough indication of grouping.

We employed three reduction strategies: None, MDS, and UMAP.

## Clustering

After dimensionality reduction, the resulting dataset can be subjected to a wide selection of clustering algorithms that each have optimal conditions (for an overview, see (Jain et al., 1999)). Here, we will explore the most common types. This includes k-means (Lloyd, 1982), an algorithm that arbitrarily draws a predefined number ( $k$ ) of centroids within the data, and on each iteration moves the centroids to the average of the observations that are closest to each centroid, until a stable solution is reached. Another approach is (hierarchical) agglomerative clustering, which recursively joins pairs of observations according to a combination of linkage affinity (e.g. Euclidean or cosine distance) and criterion. A commonly used linkage is Ward, which minimises the variance of merging groups of observations (Ward, 1963). Because these algorithms require the user to define the number of clusters, a common approach is to cycle through a variety of options to identify the best fitting solution.

A class of algorithms that does not require the prespecification of an expected number of clusters includes DBSCAN (Ester et al., 1996) and HDBSCAN (McInnes et al., 2017). They identify clusters of denser observations among lower-density observations that remain unassigned.

We employed five algorithms: k-means, agglomerative clustering with Ward linkage and Euclidean distance, agglomerative clustering with average linkage and cosine distance, HDBSCAN, and c-means (fuzzy clustering; see below).

## Outcome evaluation

After observations are assigned a cluster, the quality of the solution can be determined. For each sample, a silhouette coefficient can be computed as the relative distance to its assigned centroid and the nearest other centroid (Rousseeuw, 1987). For each observation, a value of 1 means perfect alignment with its assigned centroid, 0 means it lies exactly in between its centroid and the nearest other, and -1 means perfect alignment with a centroid it was not assigned to. The average across all assigned observations is the silhouette score, which is often taken as evidence for clustering if it exceeds 0.5, or as strong evidence if it exceeds 0.7 (Kaufman & Rousseeuw, 1990). It should be noted that there are many cluster validation indices (for excellent overviews, see (Arbelaitz et al., 2013; Vendramin et al., 2010)). We focus on the silhouette score because of its good performance in many circumstances (Arbelaitz et al., 2013), conceptual elegance, and established thresholds for interpretation.

While a ground truth is normally not available, it is in the context of simulated data. This allowed us to compute the Rand index (Rand, 1971), adjusted for chance (Hubert & Arabie, 1985), to quantify the overlap between cluster outcome and ground truth. An adjusted Rand index of 1 reflects perfect match, a value of 0 means chance performance, and negative values indicate the clustering performed worse than chance. While the adjusted Rand index quantifies the overlap between cluster outcome and truth, the silhouette coefficient reflects what an experimenter (who is normally blind to the ground truth) would conclude.

## Fuzzy clustering

We employed the c-means algorithm (Bezdek, 1981; Dunn, 1973), specifically the version implemented in Python package scikit-fuzzy (Ross, 2010). It converges on centroids in a similar way to k-means, but allows for observations to be assigned to more than one cluster. We estimated its outcomes using a variation of the silhouette coefficient intended for fuzzy clustering methods (Campello & Hruschka, 2006). This silhouette score has a tunable exponentiation parameter  $\alpha$  that determines how strongly the uncertainty about each observations cluster membership is weighted (when it approaches 0, the fuzzy silhouette coefficient approaches the regular version). It was set to 1 in our analyses.

As described above, datasets (N=120) were simulated with 1-4 subgroups (multivariate normal distributions with SD=1) with separations of  $\Delta=1$  to 10. A new dataset was simulated in 100 iterations. In each, k-means and c-means were applied, with predefined guesses of k=2 to 7. From the outcomes, we computed the probability of each analysis to detect clustering (silhouette

coefficient  $\geq 0.5$ ), and to detect the correct number of clusters (silhouette coefficient highest for the value of  $k$  that corresponded with ground truth).

## Effect of dimensionality reduction on cluster separation

In the simulated datasets, distances between cluster centroids in original feature space should be Euclidean (Equation 1). However, due to the stochastic and non-linear nature of dimensionality reduction algorithms, centroid distances after dimensionality reduction are less predictable. To quantify the effect of dimensionality reduction on cluster separation, we computed the distance between cluster centroids (defined as the average Euclidean position of observations within a cluster) in projected space after dimensionality reduction.

$$(1) \quad \Delta = \sqrt{\sum_{i=1}^n \delta_i^2}$$

Where  $\Delta$  is centroid distance,  $n$  is the number of features, and  $\delta$  is the within-feature difference between clusters (effect size).

## Introducing effect size $\Delta$

We consider multivariate normal distributions with standard deviations of 1 (for all features) to be standardised space, and refer to cluster separation in this space as  $\Delta$ . It can serve as an effect size metric for clustering in the sense that it reflects the extent of separation of simulated or identified subgroups. It is essentially the multivariate equivalent of Cohen's  $d$ , and can in fact be estimated from expected values of Cohen's  $d$  within each feature via Equation 1.

## Power and accuracy

Researchers who opt for cluster analysis are likely attempting to answer three main questions: 1) Are subgroups present in my data, 2) How many subgroups are present in my data, and 3) Which observations belong to what subgroup?

In null-hypothesis testing, power relates to the probability that a null hypothesis is correctly rejected if an alternative hypothesis is true. Various approaches have been suggested to define statistical power in cluster analyses, for example through outcome permutation (Baker & Hubert, 1975) or through measures of subgroup overlap (Sneath, 1977). Here, we define power as the likelihood of a cluster analysis to accurately reject the null hypothesis that no subgroups are present, based on the binary decision criterium of a solution's silhouette score being 0.5 or over (Kaufman & Rousseeuw, 1990).

Further to the binary decision of clusters being present in a dataset, we estimated the probability of cluster analyses to identify the correct number of subgroups in simulated datasets. This was done by cycling through  $k=2$  to  $k=5$  for algorithms that require pre-specification of cluster number ( $k$ -means and agglomerative clustering), and choosing the value that resulted in the highest

silhouette coefficient. HDBSCAN reports the number of detected clusters, and thus did not require iterating through pre-specified values.

Finally, we quantified classification accuracy as the proportion of observations correctly assigned to their respective clusters. This reflects the overlap between ground truth and assigned cluster membership. This accuracy is dependent on chance, which was set at the proportion of the total sample size that was in the largest cluster.

## Results

### Cluster centroid separation

Using the ground truth cluster membership, we computed the distance  $\Delta$  between simulated datasets' cluster centroids (after projection into two dimensions) as the Euclidean distance between the average positions of observations within each cluster in reduced space. For three-cluster datasets, we computed the distance between the “middle” cluster and another cluster's centroid to obtain the smallest between-cluster distance.

Centroid distance  $\Delta$  is plotted as a function of both within-feature effect size  $\delta$  and the proportion of different features after dimensionality reduction through MDS (Figure 2) and UMAP (Figure 3). The visualised datasets also differed in number of clusters (two unequally sized, two equally sized, or three equally sized), and covariance structure (no covariance, random covariance, or different covariances between clusters), adding up to 180 datasets per figure.

Differences between the number and size of clusters or the covariance structures is negligible for MDS. Overall, cluster separation increases as a function of higher differences between clusters within each feature, and the proportion of different features. The same is true for UMAP, although its outcomes are non-linear and more variable.

In sum, MDS dimensionality reduction shows a steady increase in cluster separation with increases in within-feature effect size and proportion of different features, whereas UMAP shows separation only at large differences (Cohen's  $d = 2.1$  within each feature) or at large proportions of different features. Crucially, clusters with different covariance structures (3-factor and 4 factor; of 3-factor, 4-factor, and random) but similar mean vectors do not show clear separation.

### d-D plots after multi-dimensional scaling (MDS)

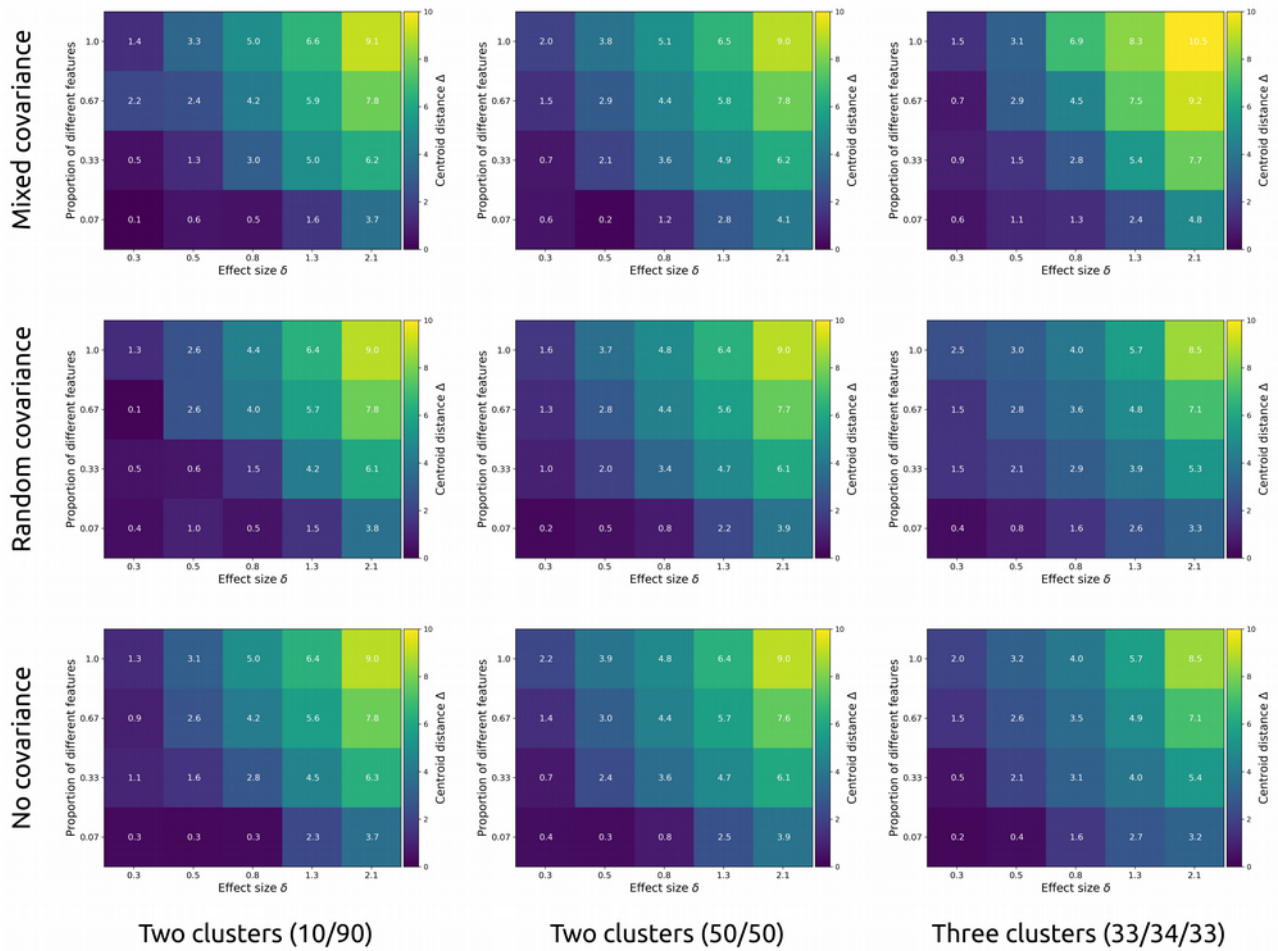


**Figure 2** – Each cell presents the cluster centroid separation  $\Delta$  (brighter colours indicate stronger separation) after multi-dimensional scaling (MDS) was applied to simulated data of 1000 observations and 15 features. Separation is shown as a function of within-feature effect size (Cohen’s  $d$ , x-axis), and the proportion of features that were different between clusters. Each row shows a different covariance structure: “mixed” indicates subgroups with different covariance structures, “random” with the same random covariance structure between all groups, and “no” for no correlation between any of the features). Each column shows a different type of population: with unequal (10 and 90%) subgroups, with two equally sized subgroups, and with three equally sized subgroups.

### d-D plots after UMAP dimensionality reduction

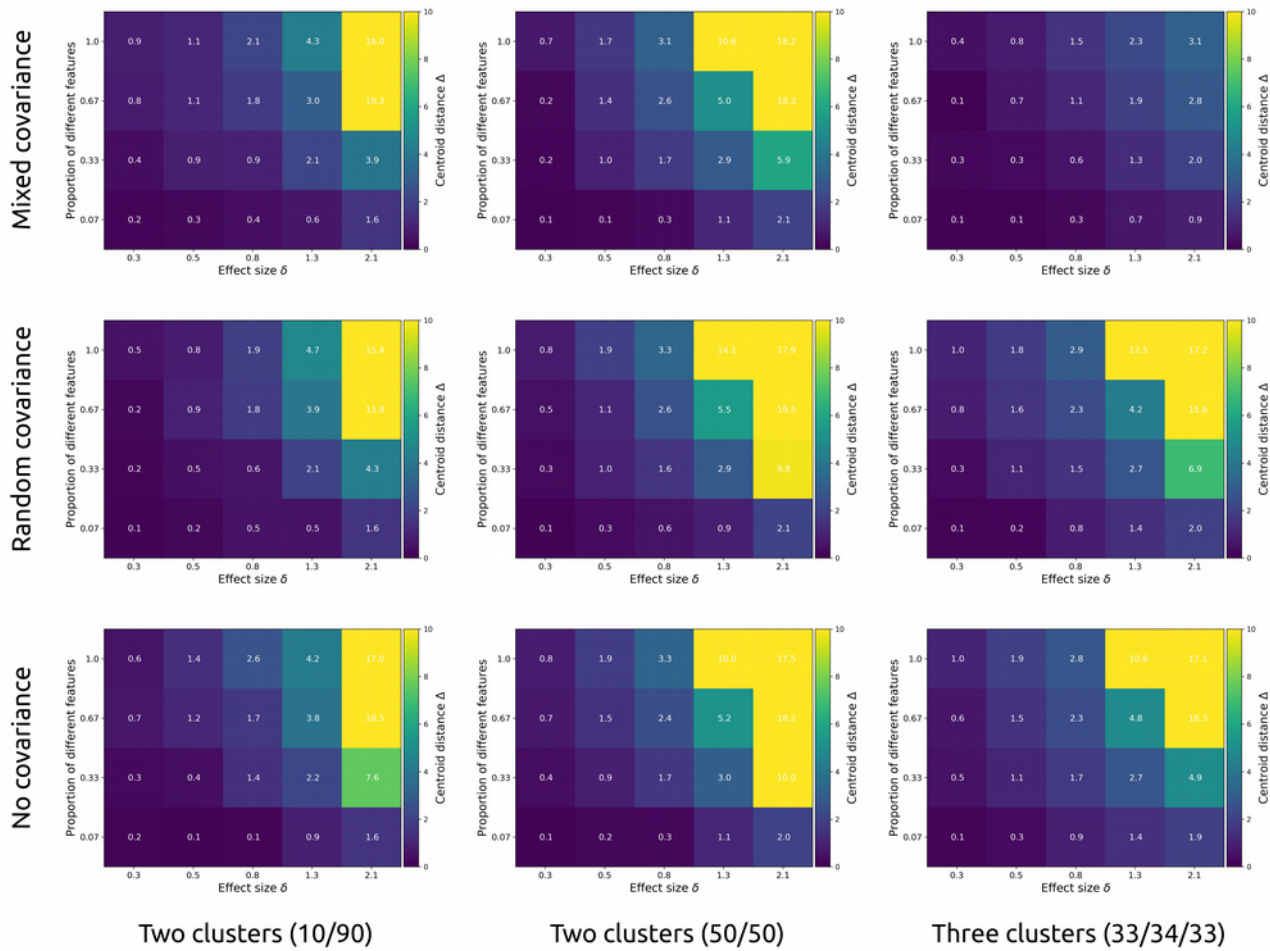


**Figure 3** – Each cell presents the cluster centroid separation  $\Delta$  (brighter colours indicate stronger separation) after uniform manifold approximation and projection (UMAP) was applied to simulated data of 1000 observations and 15 features. Separation is shown as a function of within-feature effect size (Cohen’s  $d$ , x-axis), and the proportion of features that were different between clusters. Each row shows a different covariance structure: “mixed” indicates subgroups with different covariance structures, “random” with the same random covariance structure between all groups, and “no” for no correlation between any of the features). Each column shows a different type of population: with unequal (10 and 90%) subgroups, with two equally sized subgroups, and with three equally sized subgroups.

### Membership classification (adjusted Rand index)

Overlap between clustering outcomes and ground truth was computed with the adjusted Rand index. Figure 4 shows the effects of within-feature effect size, number of different features, dimensionality reduction algorithm, and cluster algorithm on the adjusted Rand index for simulated datasets two equally sized subgroups with different covariance structures (3-factor and 4-factor).

These simulated datasets were the optimal example due to their differentiation into two equally sized groups, and their realistic difference in covariance structure.

In terms of clustering accuracy, the k-means algorithm performs roughly equally well regardless of dimensionality reduction. The same is true for the two versions of agglomerative clustering (Ward linkage with Euclidean distance, or average linkage with cosine distance). By contrast, HDBSCAN performs well only after UMAP dimensionality reduction. It is likely that this is due to the algorithm only assigning the denser centres to their respective cluster, while leaving many other observations unassigned.

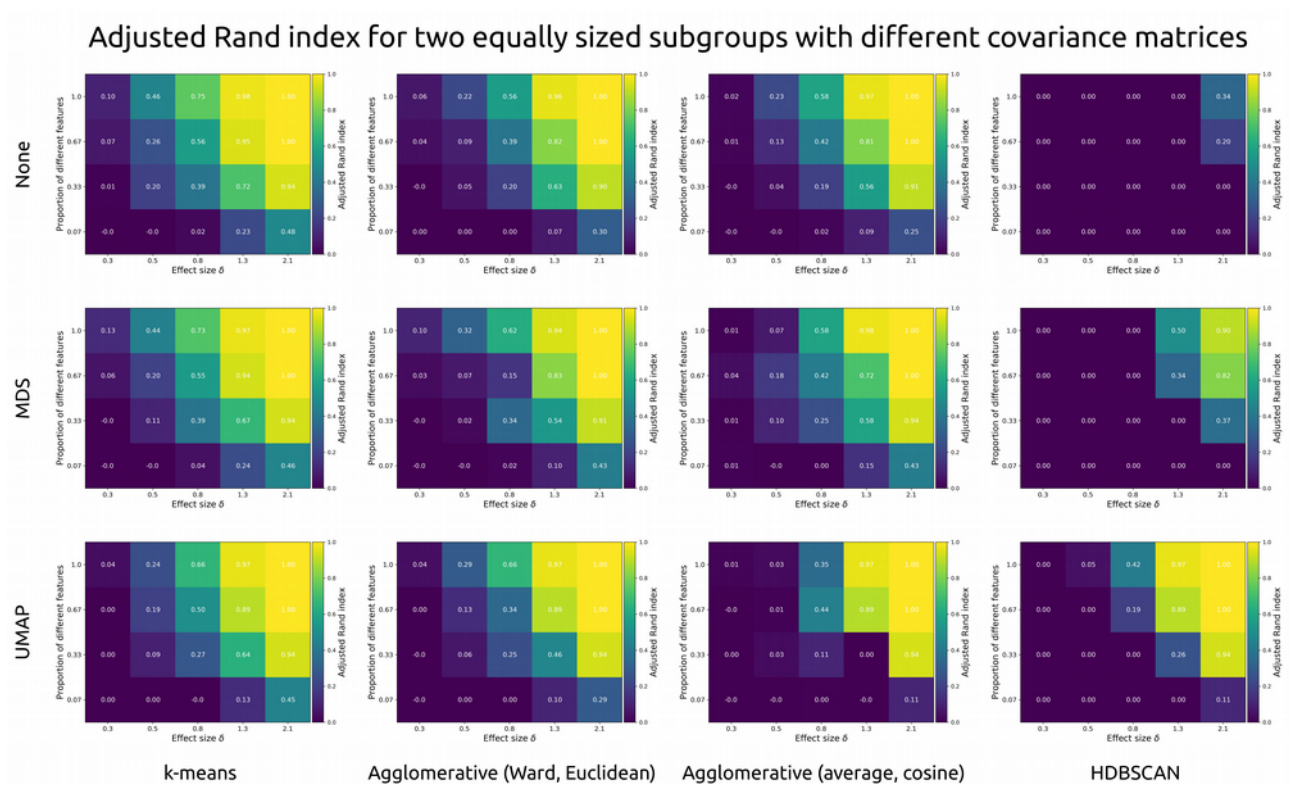


**Figure 4** – Each cell shows the adjusted Rand index (brighter colours indicate better classification) as a function of within-feature effect size (Cohen’s  $d$ ), and the proportion of features that differed between two simulated clusters with different covariance structures (3-factor and 4-factor). Each row presents a different dimensionality reduction approach: None, multi-dimensional scaling (MDS), or uniform manifold approximation and projection (UMAP). Each column presents a different type of clustering algorithm: k-means, (hierarchical) agglomerative clustering with Ward linkage and Euclidean distance, agglomerative clustering with average linkage and cosine distance, and HDBSCAN.

## Data subgrouping (silhouette coefficient)

Silhouette scores reflect the information that would have been available to a researcher to decide on whether discrete subgroups were present in the simulated datasets (i.e. without knowledge of the ground truth). Figure 5 shows the effects of within-feature effect size, number of different features, dimensionality reduction algorithm, and cluster algorithm on the silhouette scores for simulated datasets two equally sized subgroups with different covariance structures (3-factor and 4-factor). Unlike the adjusted Rand index, for which the ground truth needs to be known, silhouette scores are impacted by dimensionality reduction. Using the traditional threshold of 0.5, none of the raw datasets would have been correctly identified as clustered.

After MDS, only the datasets in which two-thirds or more of the features showed a within-feature difference with a Cohen's  $d$  of 2.1 would have been correctly identified as showing clustering through k-means and the two agglomerative clustering approaches. On the basis of HDBSCAN, a researcher would have correctly identified clustering in datasets with two-thirds or more features showing a difference with a Cohen's  $d$  of 1.3, or one-third or more features showing a difference with a Cohen's  $d$  of 2.1.

Performance is best after UMAP dimensionality reduction. Using k-means, a researcher would correctly identify the clustered nature of datasets with two-thirds of features showing differences of 0.8, or one-third or more showing differences of 1.3 or over. The same is true for HDBSCAN, which was also able to identify clustering when all features showed a within-feature difference corresponding to Cohen's  $d$  values of 0.3.

In sum, only a minority of the simulated datasets could correctly be identified as clustered, regardless of method. Dimensionality reduction, particularly the non-linear projection provided by UMAP, helped elevate cluster coefficients across the board. Only datasets with large within-feature effect sizes and a high number of features showing differences were correctly marked as "clustered" using the traditional silhouette score threshold of 0.5.

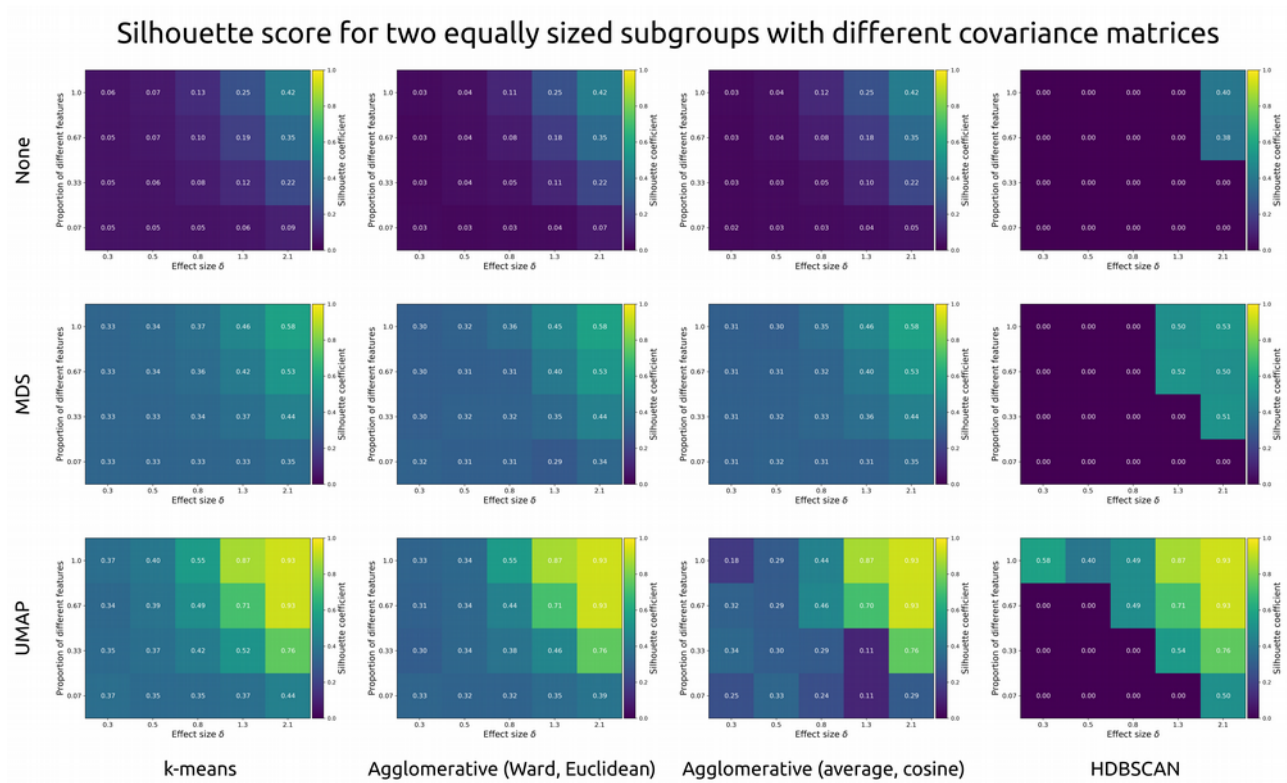


**Figure 5** – Each cell shows the silhouette coefficient (brighter colours indicate stronger detected clustering, with a threshold set at 0.5) as a function of within-feature effect size (Cohen’s  $d$ ), and the proportion of features that differed between two simulated clusters with different covariance structures (3-factor and 4-factor). Each row presents a different dimensionality reduction approach: None, multi-dimensional scaling (MDS), or uniform manifold approximation and projection (UMAP). Each column presents a different type of clustering algorithm:  $k$ -means, (hierarchical) agglomerative clustering with Ward linkage and Euclidean distance, agglomerative clustering with average linkage and cosine distance, and HDBSCAN.

## Effect of dimensionality reduction on cluster separation

As expected, simulated sample centroid distances (Figure 6, in green) were aligned with subgroup centroids before dimensionality reduction was applied, with minor random sampling error. Dimensionality reduction did impact cluster separation. MDS subtly exaggerated centroid distances across all centroid separations in original space (Figure 6, in blue). UMAP reduced sample centroid distance at lower ( $\Delta < 3$ ) and increased it at higher ( $\Delta > 4$ ) centroid distances (Figure 6, in purple). The only exception to this was the simulated dataset with three clusters of respectively 3-factor, 4-factor, and no covariance structure, where UMAP reduced centroid distance for all original centroid distances.

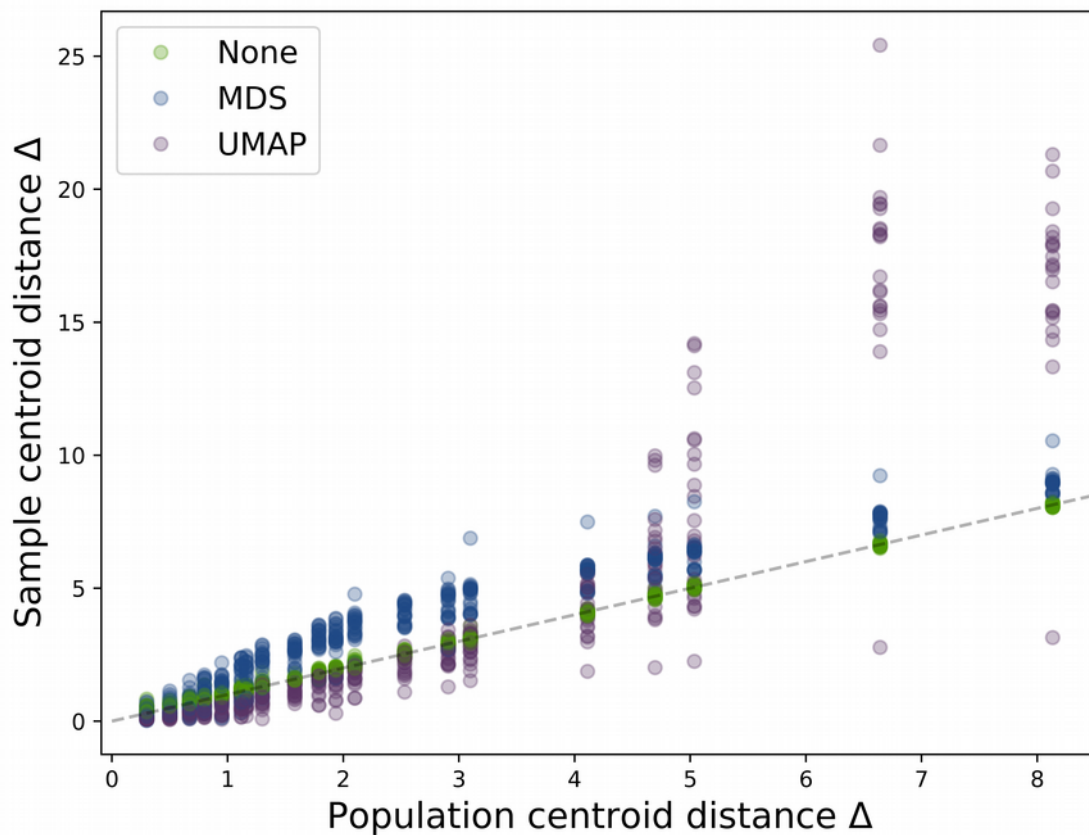


**Figure 6** – Each dot represents a simulated dataset of 1000 observations and 15 features, each with different within-feature effect size, proportion of different features between clusters, covariance structure, and number of clusters. The x-axis represents the separation between subgroups in the population that datasets were simulated from, and the y-axis represents the separation in the simulated dataset after no dimensionality reduction (green), multi-dimensional scaling (MDS, blue), or uniform manifold approximation and projection (purple). The dotted line indicates no difference between population and sample; values above the dotted line have had their separation increased, and it was decreased for those below the line.

## Statistical power and accuracy

Power was computed as the probability of correctly rejecting the null hypothesis of there not being a clustered structure to the data, which occurred when silhouette scores were 0.5 or over. The probability of selecting the correct number of clusters was computed as the proportion of solutions where the silhouette score was highest for the true number of clusters. Finally, classification accuracy was computed as the proportion of observations that was correctly assigned to their respective cluster.

## K-means

For k-means, power to detect clustering was primarily dependent on cluster separation, and much less on sample size (Table 1; Figure 7, top and second row). At cluster separation  $\Delta=5$ , there was 71% power to detect clustering in a population divided into one large (90%) and one small (10%) subgroup at sample size  $N=10$ , and 92% at  $N=20$ . For two equally sized clusters, power was 82% from separation  $\Delta=4$  at  $N=10$ , and higher for larger sample and effect sizes. For three equally sized clusters, power was 76% at separation  $\Delta=4$  for  $N=10$ , 69% for  $N=20$ , 77% to  $N=40$ , and over 80 from  $N=80$ ; with power for larger effect sizes around 100%. For four equally sized clusters, power was 75% at separation  $\Delta=4$  at  $N=80$ , 85% at  $\Delta=5$  for  $N=10$ , and around 100% for larger effect and sample sizes.

Sample sizes of  $N=40$  resulted in good (80% or higher) accuracy to detect the true number of clusters from separation  $\Delta=4$ . For equally sized clusters, that level of accuracy was also reached at separation  $\Delta=3$  when the sample size was about 20 per subgroup (Figure 7, third row).

Classification accuracy for subgroup membership of individual observations was above chance for all tested separation values and sample sizes in populations with equally sized subgroups, and above 80-90% from separation  $\Delta=3$ . Classification accuracy was above chance for populations with one small (10%) and one large (90%) subgroup from  $N=80$  and separation  $\Delta=4$  (Figure 7, bottom row).

In sum, 20 observations per subgroup resulted in sufficient power to detect the presence of subgroups with k-means, provided cluster separation was  $\Delta=4$  or over, and subgroups were roughly equally sized (detecting smaller subgroups among large subgroups was only possible for separations of  $\Delta=5$  or over). These values also provided near-perfect accuracy for the detection of the true number of clusters, and very high (90-100%) classification accuracy of individual observation's group membership.

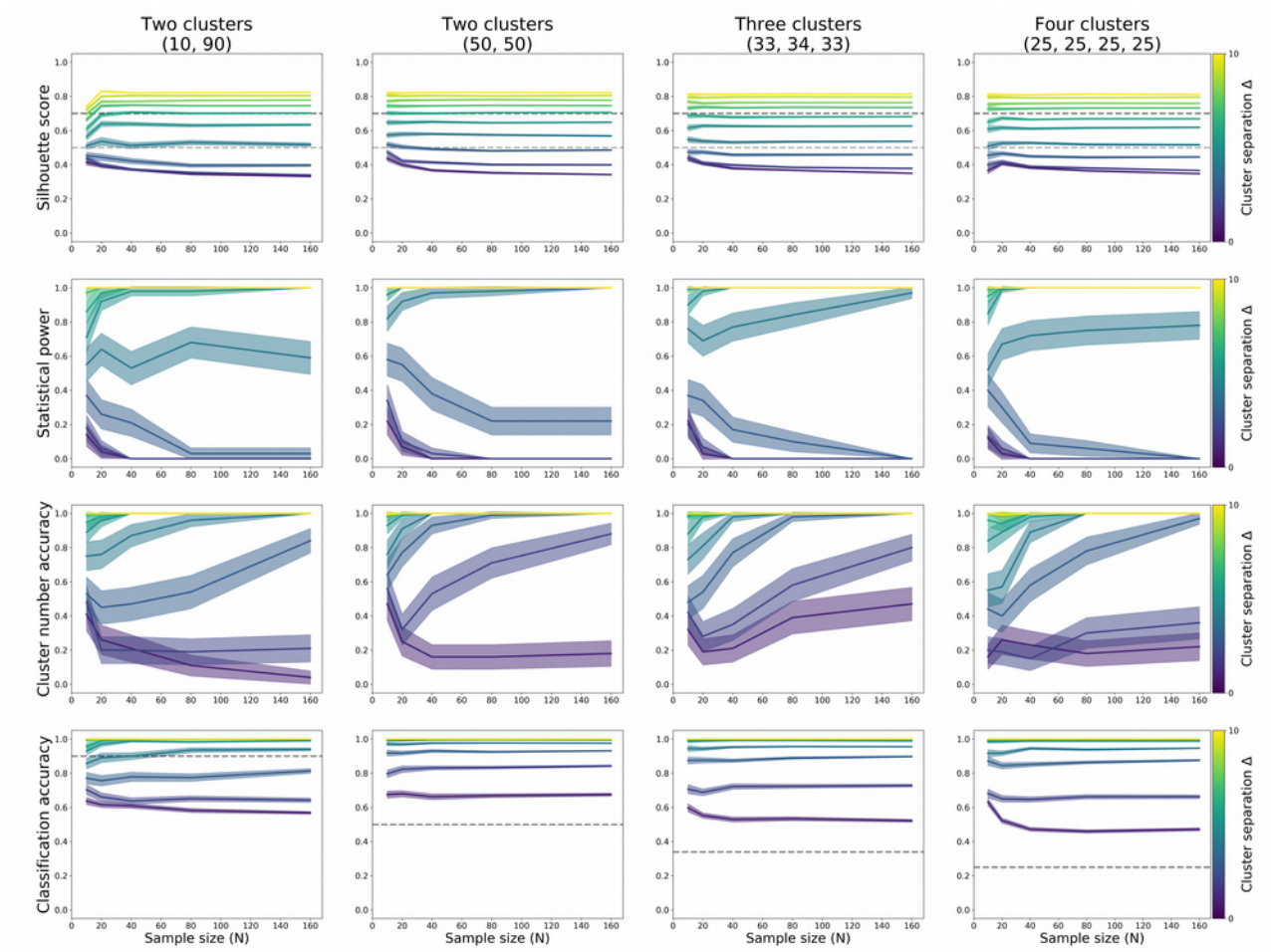


**Figure 7** – *K*-means silhouette scores (top row), proportion of correctly identified clustering (second row), proportion of correctly identified number of clusters (third row), and the proportion of observations correctly assigned to their subgroup, each computed through 100 iterations of simulation. Datasets of varying sample size (*x*-axis) and two features were sampled from populations with equidistant subgroups that each had the same 3-factor covariance structure. The simulated populations were made up of two unequally sized (10 and 90%) subgroups (left column); or two, three, or four equally sized subgroups (second, third, and fourth column, respectively).

**Table 1**

*Statistical power for the binary decision of data being “clustered” using k-means clustering. Estimates based on 100 iterations per cell, using a decision threshold of 0.5 for silhouette scores.*

	$\Delta=1$	$\Delta=2$	$\Delta=3$	$\Delta=4$	$\Delta=5$	$\Delta=6$	$\Delta=7$	$\Delta=8$	$\Delta=9$	$\Delta=10$
<b>2 Clusters</b>										
<i>(10/90%)</i>										
<b>N=10</b>	14	18	37	55	71	86	97	100	100	100
<b>N=20</b>	4	6	26	64	92	97	100	100	100	100
<b>N=40</b>	0	0	21	53	98	100	100	100	100	100
<b>N=80</b>	0	0	3	68	98	100	100	100	100	100
<b>N=160</b>	0	0	3	59	100	100	100	100	100	100
<b>2 Clusters</b>										
<i>(50/50%)</i>										
<b>N=10</b>	22	34	58	82	96	100	100	100	100	100
<b>N=20</b>	7	10	55	92	100	100	100	100	100	100
<b>N=40</b>	0	3	38	97	100	100	100	100	100	100
<b>N=80</b>	0	0	22	98	100	100	100	100	100	100
<b>N=160</b>	0	0	22	100	100	100	100	100	100	100
<b>3 Clusters</b>										
<i>(33/34/33%)</i>										
<b>N=10</b>	22	20	37	76	90	99	100	100	100	100
<b>N=20</b>	3	7	34	69	98	100	100	100	100	100
<b>N=40</b>	0	0	17	77	100	100	100	100	100	100
<b>N=80</b>	0	0	10	84	100	100	100	100	100	100
<b>N=160</b>	0	0	0	97	100	100	100	100	100	100
<b>4 Clusters</b>										
<i>(25/25/25/25%)</i>										
<b>N=10</b>	12	13	40	52	85	95	99	100	100	100
<b>N=20</b>	3	6	30	67	99	100	100	100	100	100
<b>N=40</b>	0	0	9	72	100	100	100	100	100	100
<b>N=80</b>	0	0	6	75	100	100	100	100	100	100
<b>N=160</b>	0	0	0	78	100	100	100	100	100	100

## HDBSCAN

For HDBSCAN, power to detect clustering was primarily dependent on effect size, provided the sample size was over a threshold (Table 2; Figure 8, top and second row). For a population divided into one large (90%) and one small (10%) cluster, power was 84% at  $N=80$  for separation  $\Delta=6$ . For two clusters of equal size, power was 66% at  $N=40$  and 83% for  $N=80$  for separation  $\Delta=3$ . For three clusters of equal size, power was 66% at  $N=160$  for separation  $\Delta=3$ , and 84% at  $N=80$  for separation  $\Delta=4$ . For four clusters of equal size, power was 75% at  $N=80$  for separation  $\Delta=4$ .

In addition to detecting subgrouping in the data, Figure 8 (third row) shows the probability that HDBSCAN detected the correct number of subgroups. This, too, was strongly dependent on cluster separation. Accuracy was highest for separations of  $\Delta=5$  or over, and mostly acceptable (around 70-80%) at separations  $\Delta=4$ . For equally sized clusters, this was true from  $N=40$ , while the accurate detection of one small (10%) and one large (90%) subgroup required  $N=80$  or over.

The accuracy of classifying observations' cluster membership (Figure 8, bottom row) was only over chance at from separations of  $\Delta=8$  and sample sizes of  $N=80$  for populations with one small (10%) and one large (90%) subgroup (chance = 90%). It was over chance from  $\Delta=4$  and  $N=40$  for populations with two equally sized subgroups (chance = 50%), from  $\Delta=4$  and  $N=40$  for populations with three equally sized subgroups (chance = 33%), and from  $\Delta=3$  and  $N=40$  for populations with four equally sized subgroups (chance = 25%).

In sum, 20-30 observations per subgroup resulted in sufficient power to detect the presence of subgroups with HDBSCAN, provided cluster separation was  $\Delta=4$  or over, and subgroups were roughly equally sized (detecting smaller subgroups among large subgroups was only possible for separations of  $\Delta=6$  or over). These values also provided reasonable accuracy for the detection of the true number of clusters, as well as over-chance classification accuracy of individual observation's group membership.

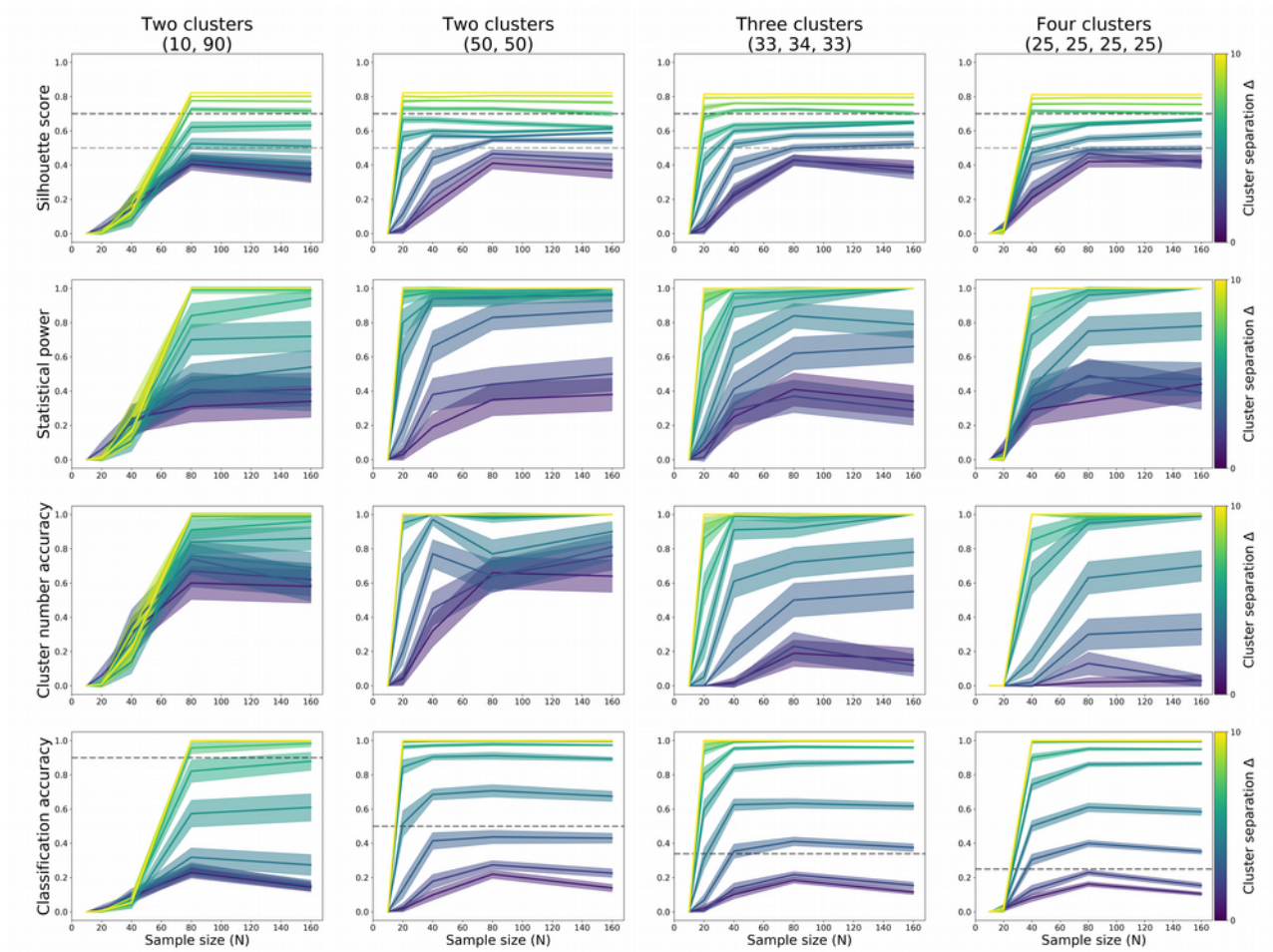


**Figure 8** – HDBSCAN silhouette scores (top row), proportion of correctly identified clustering (second row), proportion of correctly identified number of clusters (third row), and the proportion of observations correctly assigned to their subgroup, each computed through 100 iterations of simulation. Datasets of varying sample size ( $x$ -axis) and two features were sampled from populations with equidistant subgroups that each had the same 3-factor covariance structure. The simulated populations were made up of two unequally sized (10 and 90%) subgroups (left column); or two, three, or four equally sized subgroups (second, third, and fourth column, respectively).

**Table 2**

*Statistical power for the binary decision of data being “clustered” using HDBSCAN clustering. Estimates based on 100 iterations per cell, using a decision threshold of 0.5 for silhouette scores.*

	$\Delta=1$	$\Delta=2$	$\Delta=3$	$\Delta=4$	$\Delta=5$	$\Delta=6$	$\Delta=7$	$\Delta=8$	$\Delta=9$	$\Delta=10$
<b>2 Clusters</b>										
<i>(10/90%)</i>										
<b>N=10</b>	0	0	0	0	0	0	0	0	0	0
<b>N=20</b>	0	6	0	1	1	1	0	0	1	1
<b>N=40</b>	24	21	22	23	11	19	15	16	25	16
<b>N=80</b>	31	39	41	46	70	84	99	100	100	100
<b>N=160</b>	34	41	38	54	72	94	99	100	100	100
<b>2 Clusters</b>										
<i>(50/50%)</i>										
<b>N=10</b>	0	0	0	0	0	0	0	0	0	0
<b>N=20</b>	3	5	18	61	80	95	98	100	100	100
<b>N=40</b>	19	38	66	94	94	98	99	100	100	100
<b>N=80</b>	35	44	83	95	94	97	100	100	100	100
<b>N=160</b>	38	50	87	96	100	97	100	100	100	100
<b>3 Clusters</b>										
<i>(33/34/33%)</i>										
<b>N=10</b>	0	0	0	0	0	0	0	0	0	0
<b>N=20</b>	6	1	10	17	42	62	92	96	100	100
<b>N=40</b>	25	29	41	65	89	97	100	100	100	100
<b>N=80</b>	41	37	62	84	94	98	100	100	100	100
<b>N=160</b>	34	29	66	79	100	100	100	100	100	100
<b>4 Clusters</b>										
<i>(25/25/25/25%)</i>										
<b>N=10</b>	0	0	0	0	0	0	0	0	0	0
<b>N=20</b>	6	5	2	2	2	2	0	0	0	1
<b>N=40</b>	29	32	37	42	73	89	100	100	100	100
<b>N=80</b>	34	49	48	75	96	99	100	100	100	100
<b>N=160</b>	44	39	47	78	100	100	100	100	100	100

## C-means

As for k-means and HDBSCAN, for c-means power to detect clustering was primarily dependent on cluster separation, and much less on sample size (Table 3; Figure 9, top and second row). At cluster separation  $\Delta=5$ , there was 81% power to detect clustering in a population divided into one large (90%) and one small (10%) subgroup at sample size  $N=20$ , and 95-100% at larger effect and sample sizes. For two equally sized clusters, power was 77% for  $N=10$  and 82% and  $N=20$  for separation  $\Delta=3$ , and 91-100% for larger sample and effect sizes. For three equally sized clusters, power was 77% at separation  $\Delta=3$  for  $N=40$ , 76% for  $N=10$  at  $\Delta=4$ , and 89-100% for larger sample and effect sizes. For four equally sized clusters, power was 75% for  $N=40$  and 83% at  $N=80$  at separation  $\Delta=3$ , 94% for  $N=20$  at  $\Delta=4$ , and around 100% for larger effect and sample sizes.

Sample sizes of  $N=40$  resulted in good (80% or higher) accuracy to detect the true number of clusters from separation  $\Delta=4$ . For equally sized clusters, that level of accuracy was also reached at separation  $\Delta=3$  when the sample size was about 20 per subgroup (Figure 9, third row).

Classification accuracy for subgroup membership of individual observations was above chance for all tested separation values and sample sizes in populations with equally sized subgroups, and above 80-90% from separation  $\Delta=3$ . Classification accuracy was above chance for populations with one small (10%) and one large (90%) subgroup from  $N=40$  and separation  $\Delta=5$  (Figure 9, bottom row).

In sum, 20 observations per subgroup resulted in sufficient power to detect the presence of subgroups with c-means, provided cluster separation was  $\Delta=3$  or over, and subgroups were roughly equally sized (detecting smaller subgroups among large subgroups was only possible for separations of  $\Delta=5$  or over). These values also provided near-perfect accuracy for the detection of the true number of clusters, and very high (90-100%) classification accuracy of individual observation's group membership.

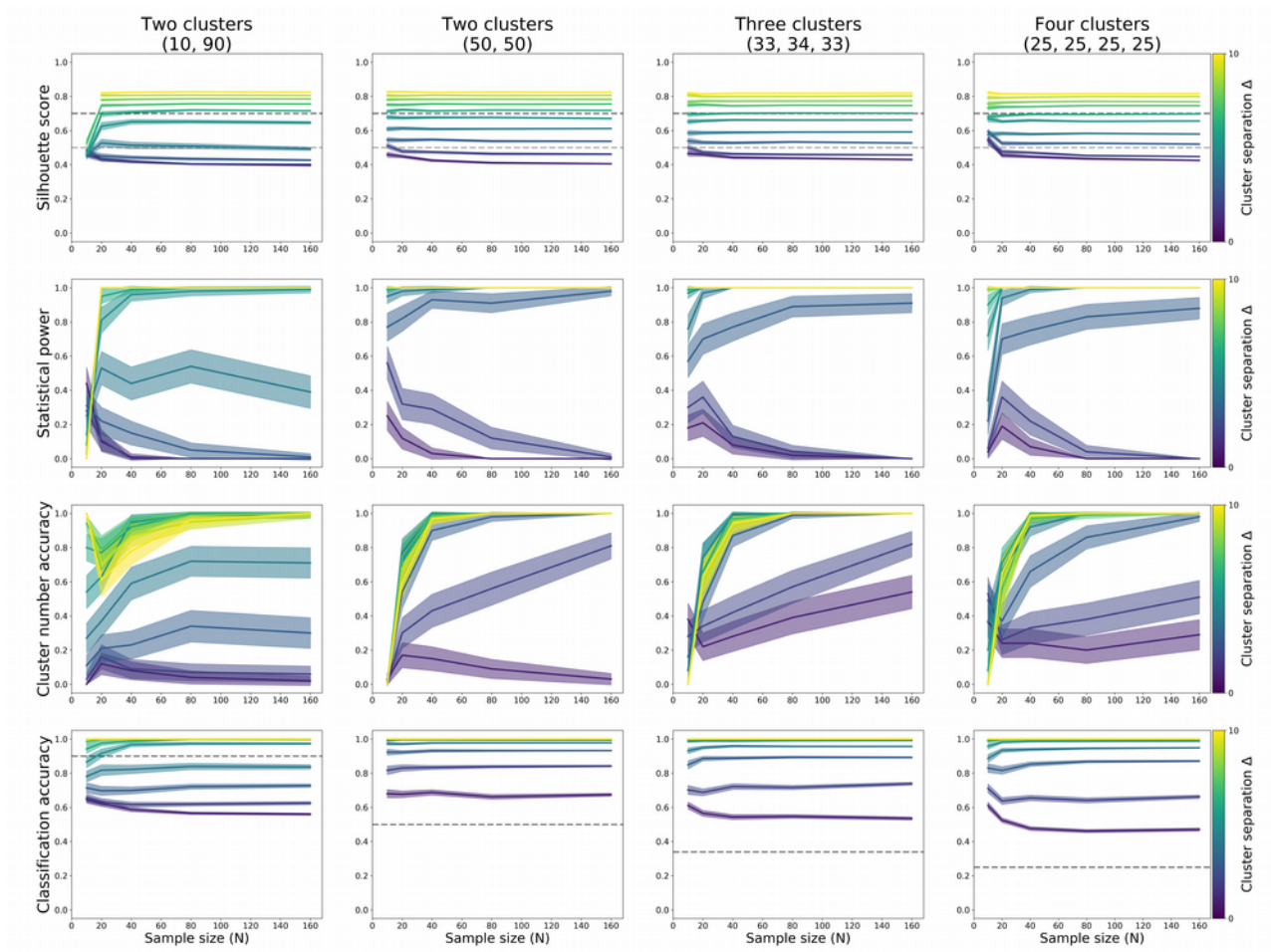


**Figure 9** – C-means silhouette scores (top row), proportion of correctly identified clustering (second row), proportion of correctly identified number of clusters (third row), and the proportion of observations correctly assigned to their subgroup, each computed through 100 iterations of simulation. Datasets of varying sample size (x-axis) and two features were sampled from populations with equidistant subgroups that each had the same 3-factor covariance structure. The simulated populations were made up of two unequally sized (10 and 90%) subgroups (left column); or two, three, or four equally sized subgroups (second, third, and fourth column, respectively).



## Direct comparison of hard k-means and fuzzy c-means

The power results summarised above suggested c-means (80-100% power at  $\Delta=3$ ) is more powerful than k-means (70-100% power at  $\Delta=4$ ) for detecting equally sized clusters. However, k-means outcomes were interpreted using the traditional silhouette score, whereas c-means was using the fuzzy silhouette score. It could be that the latter simply inflates silhouette scores, which would make c-means more likely to detect clustering  $\Delta=3$  and 4 (see Figure 10 for an example). However, such an inflation could also increase the likelihood of false positives. Hence, we simulated data without clustering ( $k=1$ ), and data with equidistant clusters of equal size ( $k=2$  to 4) with a range of separations ( $\Delta=1$  to 10).

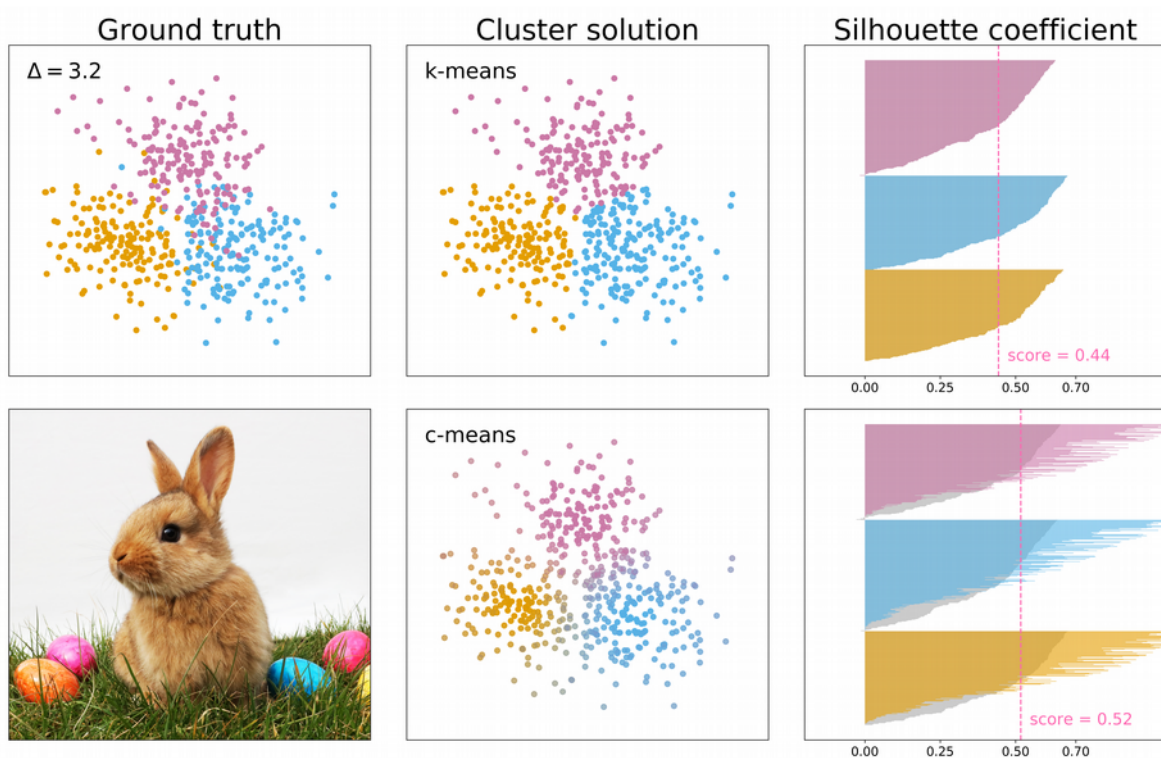


**Figure 10** – Clustering outcomes of hard k-means clustering (top row) and fuzzy c-means clustering (bottom row). The top-left panel shows the ground truth, a sample ( $N=600$ ) from a simulated population made up of three equally sized and equidistant subgroups. The middle column shows the assignment of observations to clusters, and the right column shows the corresponding silhouette coefficients. The shading in the bottom silhouette plot indicates the “hard” clustering silhouette coefficients, and the coloured bars indicate a transformation equivalent to that performed to compute the fuzzy silhouette score. The bottom-left shows a bunny (also fuzzy) amid contained and well-separated ellipsoidal clusters (photo by Tim Reckmann, licensed CC-BY 2.0).

Fuzzy silhouette scores were indeed inflated, but only for lower cluster separations (Figure 11). Furthermore, the probability of c-means fuzzy silhouette scores to surpass the 0.5 threshold when no clustering was present was only 1%, a negligible difference from 0% for k-means (Figure 11, left column; based on 100 iterations; using the algorithms on the same simulated data in each). In sum, c-means and the fuzzy cluster coefficient increase the likelihood of cluster detection, but not the false positive rate.

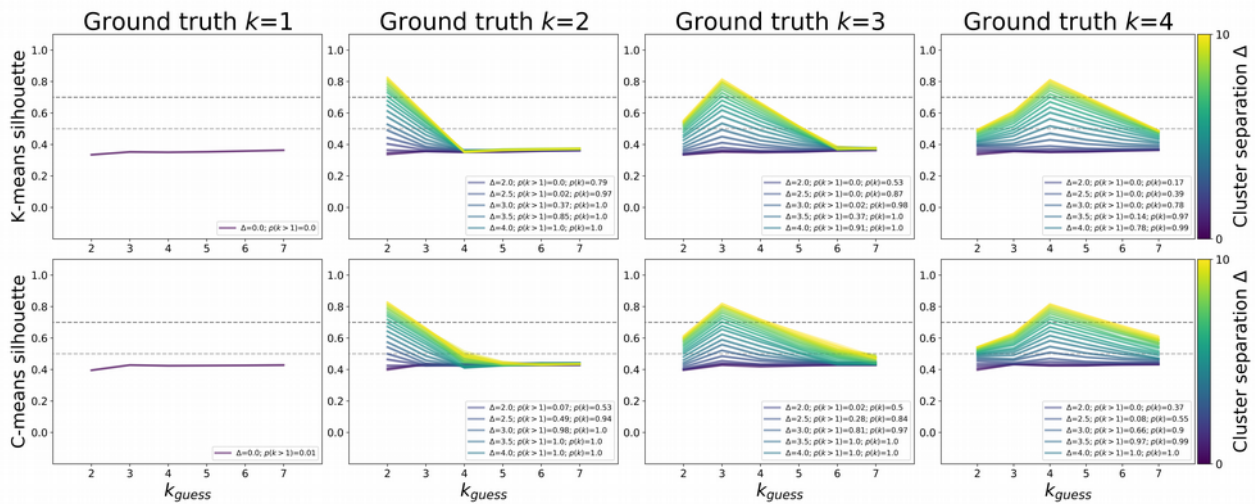


**Figure 11** – Traditional (top row) and fuzzy (bottom row) silhouette scores, respectively computed after k-means and c-means clustering. Each line presents the mean and 95% confidence interval obtained over 100 iterations of sampling ( $N=120$ , two uncorrelated features) from populations with no subgroups (left column), two subgroups (second column), three subgroups (third column), or four subgroups (right column) that were equidistant and of equal size. The same dataset in each iteration was subjected to both k-means and c-means. Estimates were obtained for different centroid separation values ( $\Delta=1$  to 10, in steps of 0.5; brighter colours indicate stronger separation). All simulation results are plotted, and the most distinct values ( $\Delta=2$  to 4) between the two algorithms are annotated.

## Discussion

Ensuring adequate statistical power is essential to improve reliability and replicability of science (Button et al., 2013; Ioannidis, 2005; Nord et al., 2017). We employed a simulation approach to determining statistical power for cluster analyses, i.e. the probability of correctly accepting the hypothesis that subgroups exist in multivariate data. We simulated subgroups as multivariate normal distributions that varied in number, relative size, separation, and covariance structure. We also varied dimensionality reduction technique. We found that covariance structure did not impact cluster analysis outcomes. Dimensionality reduction through multi-dimensional scaling (MDS) increases subgroup separation by about  $\Delta=1$ , whereas uniform manifold approximation and projection (UMAP) decreases separation when it was below  $\Delta=4$  in original space, or increase it when original separation was over  $\Delta=5$ . While centroid separation is the main driver of statistical power in cluster analysis, sample size and relative subgroup size had some effect. In populations with a small subgroup (10%), larger separation was required to properly detect clustering. Furthermore, most algorithms performed optimally at lower separations only with a minimum sample size of 20-30 observations per subgroup, and thus a total sample size of that multiplied by the number of subgroups ( $k$ ) that (are expected to) exist within the population. Practical suggestions for researchers are summarised below.

## Take-home messages

Cluster analyses are not sensitive to covariance structure, or differences in covariance structure between subgroups.

If you are testing the hypothesis that subgroups with different means exist within your population, cluster analysis will only be able to confirm this if the groups show strong separation. You can compute the expected separation in your data using Equation 1. Suppose you measure 100 features in a population that constitutes two equally sized subgroups that show a small differences (Cohen's  $d = 0.3$ ) in 20 features, medium differences (Cohen's  $d = 0.5$ ) in 12, and large differences (Cohen's  $d = 0.8$ ) in 4, your total separation should be  $\Delta=2.7$ .

Dimensionality reduction through MDS subtly increases separation  $\Delta$  by about 1 in our simulations, and hence can help improve your odds of accurately detecting clustering. By contrast, dimensionality reduction UMAP will underestimate cluster separation if separation in original feature space is below  $\Delta=4$ , but it will strongly increase cluster separation for original separation values over 5. Hence, in the context of multivariate normal distributions, we would recommend using MDS. In our previous example of an original separation of  $\Delta=2.7$ , our simulations suggested this would increase to between 4 and 5 through MDS, or remain the same or decrease slightly through UMAP.

Provided subgroups are sufficiently separated in your data ( $\Delta=4$ ), sampling at least  $N=20-30$  observations per group will provide sufficient power to detect subgrouping with k-means or

HDBSCAN, with decent accuracy for both the detection of the number of clusters in your sample, and the classification of individual observations' cluster membership.

Finally, using c-means and its fuzzy cluster score could improve the power of cluster analyses without elevating the false positive rate. This is particularly useful if the expected cluster centroid separation is between  $\Delta=3$  and 4, where k-means is less likely to reliably detect subgroups.

## Conclusion

Cluster algorithms have sufficient statistical power to detect subgroups (multivariate normal distributions with different centres) only when these are sufficiently separated. Specifically, the separation in standardised space (here named effect size  $\Delta$ ) should be at least 4 for k-means and HDBSCAN to achieve over 80% power. Better power is observed for c-means, which achieved 80% power at  $\Delta=3$  without associated inflation of the false positive rate. This effect size can be computed as the accumulation of expected within-feature effect sizes. While covariance structure did not impact clustering, sample size did to some extent, particularly for HDBSCAN and k-means. Sampling at least  $N=20$  to 30 per expected subgroup resulted in satisfactory results.

## References

- Arbelaitz, O., Gurrutxaga, I., Muguerza, J., Pérez, J. M., & Perona, I. (2013). An extensive comparative study of cluster validity indices. *Pattern Recognition*, *46*(1), 243–256.  
<https://doi.org/10.1016/j.patcog.2012.07.021>
- Astle, D. E., Bathelt, J., The CALM Team, & Holmes, J. (2019). Remapping the cognitive and neural profiles of children who struggle at school. *Developmental Science*, *22*(1), e12747.  
<https://doi.org/10.1111/desc.12747>
- Baker, F. B., & Hubert, L. J. (1975). Measuring the Power of Hierarchical Cluster Analysis. *Journal of the American Statistical Association*, *70*(349), 31–38.
- Bathelt, J., Holmes, J., Astle, D. E., & The CALM Team. (2018). Data-Driven Subtyping of Executive Function–Related Behavioral Problems in Children. *Journal of the American Academy of Child & Adolescent Psychiatry*, *57*(4), 252-262.e4.  
<https://doi.org/10.1016/j.jaac.2018.01.014>

- Bathelt, J., Johnson, A., Zhang, M., the CALM team, & Astle, D. E. (2017). *Data-driven brain-types and their cognitive consequences* [Preprint]. Neuroscience.  
<https://doi.org/10.1101/237859>
- Bellman, R. (1957). *Dynamic programming*. Princeton University Press.
- Benjamins, J. S., Dalmaijer, E. S., Ten Brink, A. F., Nijboer, T. C. W., & Van der Stigchel, S. (2019). Multi-target visual search organisation across the lifespan: cancellation task performance in a large and demographically stratified sample of healthy adults. *Aging, Neuropsychology, and Cognition*, 26(5), 731–748. <https://doi.org/10.1080/13825585.2018.1521508>
- Bezdek, J. C. (1981). *Pattern recognition with fuzzy objective function algorithms*. Plenum Press.
- Button, K. S., Ioannidis, J. P. A., Mokrysz, C., Nosek, B. A., Flint, J., Robinson, E. S. J., & Munafò, M. R. (2013). Power failure: why small sample size undermines the reliability of neuroscience. *Nature Reviews Neuroscience*, 14(5), 365–376.  
<https://doi.org/10.1038/nrn3475>
- Campello, R. J. G. B., & Hruschka, E. R. (2006). A fuzzy extension of the silhouette width criterion for cluster analysis. *Fuzzy Sets and Systems*, 157(21), 2858–2875.  
<https://doi.org/10.1016/j.fss.2006.07.006>
- Dalmaijer, E. S. (2017). *Python for experimental psychologists*. Routledge.
- De La Monte, S. M., Moore, W. M., & Hutchins, G. M. (1986). Metastatic behavior of prostate cancer: Cluster analysis of patterns with respect to estrogen treatment. *Cancer*, 58(4), 985–993.
- Dubes, R. C. (1987). How many clusters are best? - An experiment. *Pattern Recognition*, 20(6), 645–663. [https://doi.org/10.1016/0031-3203\(87\)90034-3](https://doi.org/10.1016/0031-3203(87)90034-3)
- Dunn, J. C. (1973). A Fuzzy Relative of the ISODATA Process and Its Use in Detecting Compact Well-Separated Clusters. *Journal of Cybernetics*, 3(3), 32–57.  
<https://doi.org/10.1080/01969727308546046>
- Ester, M., Kriegel, H.-P., Sander, J., & Xu, X. (1996). A density-based algorithm for discovering clusters in large spatial databases with noise. *KDD*, 96(34), 226–231.

- Fisher, R. A. (1936). The use of multiple measurements in taxonomic problems. *Annals of Eugenics*, 7(2), 179–188. <https://doi.org/10.1111/j.1469-1809.1936.tb02137.x>
- Handelsman, D. J., Teede, H. J., Desai, R., Norman, R. J., & Moran, L. J. (2017). Performance of mass spectrometry steroid profiling for diagnosis of polycystic ovary syndrome. *Human Reproduction*, 32(2), 418–422. <https://doi.org/10.1093/humrep/dew328>
- Hennig, C. (2015). What are the true clusters? *Pattern Recognition Letters*, 64, 53–62. <https://doi.org/10.1016/j.patrec.2015.04.009>
- Hennig, C. (2020). *fpc* (Version 2.2-5) [Computer software]. <https://cran.r-project.org/web/packages/fpc/index.html>
- Hubert, L., & Arabie, P. (1985). Comparing partitions. *Journal of Classification*, 2(1), 193–218. <https://doi.org/10.1007/BF01908075>
- Ioannidis, J. P. A. (2005). Why Most Published Research Findings Are False. *PLoS Medicine*, 2(8), e124. <https://doi.org/10.1371/journal.pmed.0020124>
- Jain, A. K., Murty, M. N., & Flynn, P. J. (1999). Data clustering: a review. *ACM Computing Surveys (CSUR)*, 31(3), 264–323. <https://doi.org/10.1145/331499.331504>
- Jonsson, P. F., Cavanna, T., Zicha, D., & Bates, P. A. (2006). Cluster analysis of networks generated through homology: automatic identification of important protein communities involved in cancer metastasis. *BMC Bioinformatics*, 7(1), 2. <https://doi.org/10.1186/1471-2105-7-2>
- Kaufman, L., & Rousseeuw, P. J. (Eds.). (1990). *Finding Groups in Data*. John Wiley & Sons, Inc. <https://doi.org/10.1002/9780470316801>
- Kruskal, J. (1964). Multidimensional scaling by optimizing goodness of fit to a nonmetric hypothesis. *Psychometrika*, 29(1), 1–27.
- Lloyd, S. P. (1982). Least squares quantization in PCM. *IEEE Transactions on Information Theory*, 28(2), 129–137.
- McInnes, L., Healy, J., & Astels, S. (2017). hdbscan: Hierarchical density based clustering. *The Journal of Open Source Software*, 2(11), 205. <https://doi.org/10.21105/joss.00205>

- McInnes, L., Healy, J., & Melville, J. (2018). UMAP: Uniform Manifold Approximation and Projection for Dimension Reduction. *ArXiv:1802.03426 [Cs, Stat]*.  
<http://arxiv.org/abs/1802.03426>
- Nord, C. L., Valton, V., Wood, J., & Roiser, J. P. (2017). Power-up: A Reanalysis of “Power Failure” in Neuroscience Using Mixture Modeling. *The Journal of Neuroscience*, 37(34), 8051–8061. <https://doi.org/10.1523/JNEUROSCI.3592-16.2017>
- Oliphant, T. E. (2007). Python for Scientific Computing. *Computing in Science & Engineering*, 9(3), 10–20. <https://doi.org/10.1109/MCSE.2007.58>
- Pedregosa, F., Varoquaux, G., Gramfort, A., Michel, V., Thirion, B., Grisel, O., Blondel, M., Prettenhofer, P., Weiss, R., Dubourg, V., Vanderplas, J., Passos, A., Cournapeau, D., Brucher, M., Perrot, M., & Duchesnay, E. (2011). Scikit-learn: Machine learning in Python. *Journal of Machine Learning Research*, 12, 2825–2830.
- Rand, W. M. (1971). Objective criteria for the evaluation of clustering methods. *Journal of the American Statistical Association*, 66, 846–850.
- Rennie, J. P., Zhang, M., Hawkins, E., Bathelt, J., & Astle, D. E. (2019). Mapping differential responses to cognitive training using machine learning. *Developmental Science*.  
<https://doi.org/10.1111/desc.12868>
- Ross, T. J. (2010). Chapter 10: Fuzzy Classification (subheading: Fuzzy c-Means Algorithm). In *Fuzzy logic with engineering applications* (3rd ed., pp. 352–353). Wiley.
- Rousseeuw, P. (1987). Silhouettes: A graphical aid to the interpretation and validation of cluster analysis. *Journal of Computational and Applied Mathematics*, 20, 53–65.  
[https://doi.org/10.1016/0377-0427\(87\)90125-7](https://doi.org/10.1016/0377-0427(87)90125-7)
- Sneath, P. H. (1977). A method for testing the distinctness of clusters: a test of the disjunction of two clusters in Euclidean space as measured by their overlap. *Mathematical Geology*, 7(2), 123–143.
- Van der Maaten, L. J. P., & Hinton, G. E. (2008). Visualizing high-dimensional data using t-SNE. *Journal of Machine Learning Research*, 9, 2579–2605.
- Van Rossum, G., & Drake, F. L. (2011). *Python Language reference manual*. Network Theory Ltd.

Vendramin, L., Campello, R. J. G. B., & Hruschka, E. R. (2010). Relative clustering validity criteria: A comparative overview. *Statistical Analysis and Data Mining*, n/a-n/a.

<https://doi.org/10.1002/sam.10080>

Ward, J. H. (1963). Hierarchical Grouping to Optimize an Objective Function. *Journal of the American Statistical Association*, 58(301), 236–244.